Bulletin of Earthquake Engineering (2022) 20:4367–4393
https://doi.org/10.1007/s10518-022-01375-2

S.I. : SEISMIC STRUCTURAL HEALTH MONITORING

The value of seismic structural health monitoring for post-earthquake building evacuation

Pier Francesco Giordano[1] · Chiara Iacovino[2] · Said Quqa[3] · Maria Pina Limongelli[1]

Received: 3 August 2021 / Accepted: 26 February 2022 / Published online: 25 March 2022

Abstract
In the aftermath of a seismic event, decision-makers have to decide quickly among alternative management actions with limited knowledge on the actual health condition of buildings. Each choice entails different direct and indirect consequences. For example, if a building sustains low damage in the mainshock but people are not evacuated, casualties may occur if aftershocks lead the structure to fail. On the other hand, the evacuation of a structurally sound building could lead to unnecessary financial losses due to business and occupancy interruption. A monitoring system can provide information about the condition of the building after an earthquake that can support the choice between several competing alternatives, targeting the minimization of consequences. This paper proposes a framework for quantifying the benefit of installing a permanent seismic structural health monitoring (S^2HM) system to support building evacuation operations after a seismic event. Decision-makers can use this procedure to preventively evaluate the benefit of an SHM system and decide about the worthiness of its installation.

Keywords Value of information · Seismic structural health monitoring · Emergency management · Seismic fragility · Buildings · Indirect cost

✉ Pier Francesco Giordano
pierfrancesco.giordano@polimi.it

Chiara Iacovino
chiara.iacovino@vigilfuoco.it

Said Quqa
said.quqa2@unibo.it

Maria Pina Limongelli
mariagiuseppina.limongelli@polimi.it

[1] Department of Architecture, Built Environment and Construction Engineering, Politecnico di Milano, 20133 Piazza Leonardo da Vinci 32, Milan, Italy

[2] Department of Firefighters, Public Rescue and Civil Defense, Rome, Italy

[3] Department of Civil, Chemical, Environmental, and Materials Engineering, University of Bologna, Viale del Risorgimento 2, 40136 Bologna, Italy

1 Introduction

In the context of earthquake loss modeling, downtime is generally defined as the time between the occurrence of an earthquake and the re-occupancy of a building. It includes both an irrational and a rational component (Cardone et al. 2019). Specifically, the irrational component is the time required to assess the state of the building, take decisions, and mobilize economic and human resources. The duration of this phase depends on the dimension of the area invested by the earthquake, the density of the built environment, and the resources available to perform the inspections. The rational component, instead, includes the time to repair or replace the building, if required. In the time interval between the main seismic shock and the inspection, emergency management is particularly challenging due to the uncertainty of the structural state. However, the decision-maker should promptly decide whether evacuate the building and suspend ordinary activities or not (Han et al. 2016; Thöns and Stewart 2020).

Due to emerging signal processing techniques and improvements in sensing systems that enable the acquisition of high-fidelity dynamic measurements at the occurrence of earthquakes, Seismic Structural Health Monitoring (S^2HM) has grown considerably in the last few decades (Limongelli and Çelebi 2019). Specifically, S^2HM algorithms generally identify and track structural damage-sensitive features [e.g., inter-story drifts (Dolce et al. 2017), resonant frequencies (Iacovino et al. 2018), or nonlinear normal mode shapes (Quqa et al. 2021)] calculated instantaneously in the time interval of the strong motion. These features can be directly employed to detect and possibly localize damage induced by the seismic event or used to update finite element models (Shiradhonkar and Shrikhande 2011; Bursi et al. 2018). S^2HM may be particularly convenient compared to continuous Structural Health Monitoring (SHM) due to its robustness to temperature effects (Limongelli and Çelebi 2019). Although monitoring systems are becoming widespread for the integrity assessment of strategic and monumental structures, it is unclear if the investment, consisting of the cost of monitoring systems, is worthy. Therefore, decision-makers need tools to estimate the benefit of S^2HM before its adoption.

The Value of Information (VoI) from Bayesian decision theory can be used for this purpose (Raiffa and Schlaifer 1961; Benjamin and Cornell 1970). It can be used to quantify the amount of money saved by the decision-maker when they use the information from monitoring systems to support their decisions. Therefore, it can be intended as the maximum amount of money that the decision-maker should invest for structural health information (Pozzi and Der Kiureghian 2011; Thöns and Faber 2013; Straub 2014; Thöns 2018).

The literature on the VoI in civil engineering mainly addresses bridges and wind turbine support structures (Zhang et al. 2021). The value of collecting information on the structural health of building to support seismic emergency management operations has been addressed in (Yeo 2005) and (Omenzetter et al. 2016). In particular, (Yeo 2005) applied the classical framework of VoI from Bayesian decision analysis to assess if the collection of information on structural conditions from a visual inspection is financially desirable in managing buildings affected by earthquakes. More recently, (Omenzetter et al. 2016) discussed the VoI from the joint utilization of SHM and visual inspection information.

In general terms, the VoI is obtained by comparing two situations, namely the situation in which the decision analysis is carried out using the available information on the state of the building at the time of the decision, the so-called "Prior" decision analysis, and the situation in which the decision analysis is performed considering the new information (before having it), referred to as "Pre-Posterior" decision analysis. Both decision

analyses consist in the selection of the optimal action (e.g., between "Evacuate" or "Do not evacuate" the building), that is the one entailing the minimum expected costs. Usually, these costs depend on the probability that the damaged structure fails after selecting the action. The new information is modeled through likelihood functions, which express the probability of observing a certain monitoring outcome when the structure is in a given damage state.

In the case of seismic emergency management (Giordano and Limongelli 2020; Iannacone et al. 2021), the prior information on the structural conditions can be retrieved by so-called fragility curves, which provide the probability of reaching or exceeding a specified limit state as a function of the intensity of the damaging event. Considering aftershocks as a possible cause of the failure, the probability of failure can be obtained employing aftershock fragility functions, which express the probability of failure as a function of both the intensity of the damaging event (aftershock) and the state of the structure damaged by the mainshocks. Figure 1 shows the general flowchart of the VoI in this context, in which the decision-maker must make two decisions, namely, either installing or not the SHM system, and, if an earthquake occurs, evacuating or not the building considering aftershocks as a possible cause of the failure. If an S^2HM system is installed, it can support decision-making in the aftermath of the earthquake; otherwise, the decision-maker selects the optimal emergency management action using their available knowledge. The main elements of a VoI analysis in this context are highlighted in the figure, i.e., the (mainshocks and aftershocks) fragility functions of the considered building, the seismic hazard model of the region, the direct and indirect costs of different decision alternatives (e.g., failure/loss of functionality), and the likelihood functions in the considered damage states.

This paper intends to fill the above-mentioned research gap in the VoI literature by providing a comprehensive framework to quantify the VoI from S^2HM in building management and investigate in which cases the monitoring information provides the maximum benefit in this context. The methodology is demonstrated using a reference case study consisting of a Reinforced Concrete (RC) building located in a seismic area. Three different heights of the building have been considered to investigate the sensitivity of the VoI to this parameter. As previously remarked, the estimation of the prior probabilities of the damage states requires the availability of aftershock fragility curves. Their evaluation has

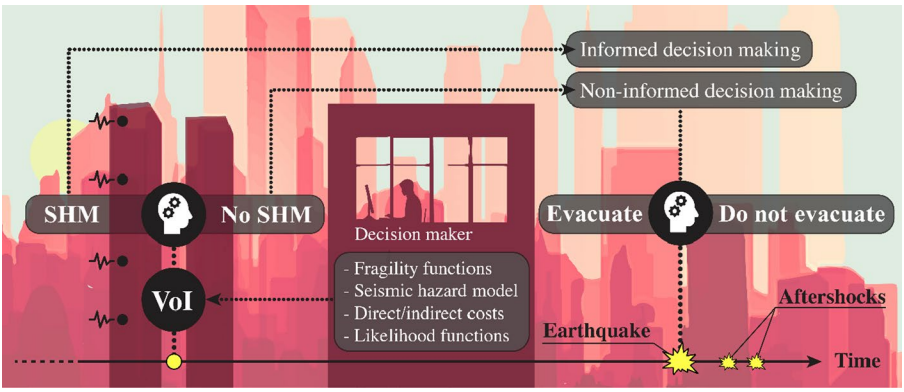

Fig. 1 VoI flowchart

received limited attention in literature thereby the relevant literature on the topic is shortly overviewed.

The paper is organized as follows. Section 2 introduces mainshock and aftershock fragility functions, Sect. 3 presents S^2HM parameters used to assess the performance of buildings in seismic prone areas. Section 4 is devoted to the description of the theoretical framework of the VoI. The reference case study is analyzed and discussed in Sect. 5, including different sensitivity analyses. The final remarks conclude the paper.

2 Seismic fragility

2.1 Mainshock fragility

The decisional framework adopted in this paper to compute the VoI from S^2HM assumes that the prior knowledge on the structural conditions of buildings in the aftermath of a seismic event is derived from fragility functions (Kassem et al. 2020; Iacovino et al. 2021) which express the probability that an Engineering Demand Parameter (EDP)—e.g., peak inter-story drift—exceeds a threshold EDP_l related to the lth damage state of the structure DS_l, given the intensity measure I_m of the mainshock. Fragility curves are generally expressed in the form:

$$P\left(EDP \geq EDP_l \middle| I_m\right) = \Phi\left[\frac{1}{\beta_{tot}} \ln\left(\frac{I_m}{I_{DS_l}}\right)\right] \tag{1}$$

where Φ is the cumulative distribution function of the standard normal distribution, I_{DS_l} and β_{tot} are respectively the median value and the dispersion of the structural capacity associated with the considered limit state (represented by the value EDP_l of the EDP). In particular, β_{tot} is the total standard deviation which represents the uncertainties in the fragility function, calculated by combining the uncertainty of the demand (intensity measure) and capacity. This latter dispersion includes model, material, and geometric uncertainties.

The intensity measure is quantified in the literature using different intensity parameters corresponding to peak (e.g., PGA, PGV, PGD) or spectral [e.g., $Sa(T)$, $Sv(T)$, $Sd(T)$] intensity measures. Fragility curves are constructed for selected damage states DS_l, identifying different performance levels of the structure. The number of damage states (and consequently the number of limit states) depends on the damage scale used. For example, the HCR (Rossetto and Elnashai 2003) damage scale considers seven different DS_l (none, slight, light, moderate, extensive, partial failure, and failure) whereas five DS_l (no damage, slight damage, moderate damage, extensive damage and failure) are defined by HAZUS99 (FEMA-NIBS 2012).

2.2 Aftershock fragility

Buildings in seismically active regions could be subjected to more than one earthquake or mainshock-aftershock sequence in a short period. Structures that present minor damage after a mainshock can be severely damaged as a result of these sequences. Aftershock fragility curves consider that, at the occurrence of the aftershock, the structure might be already in a damaged state DS_l, induced by the mainshock. With specific regard to the limit state of failure, the conditional probability that the structure (which is in a damaged state

DS_l after the mainshock) fails due to an aftershock with an intensity measure I_a can be computed as:

$$P\left(F|I_a, DS_l\right) = \Phi\left[\frac{1}{\beta_{tot}} \ln\left(\frac{I_a}{I_{F(DS_l)}}\right)\right] \tag{2}$$

where $I_{F(DS_l)}$ and β_{tot} are, respectively, the median value and the dispersion of the structural capacity associated with failure when the structure is in a damaged state DS_l at the occurrence of the aftershock. The statistical properties of I_a depend on those of the mainshock.

There is ongoing research to assess the increased seismic vulnerability of damaged structures. To understand the structural behavior under earthquake sequences, some studies use nonlinear Multiple-Degree-of-Freedom (MDOF) models (Li et al. 2014), while many others employ Single-Degree-of-Freedom (SDOF) models (Hatzigeorgiou and Beskos 2009).

In recent research works, fragility relationships are derived by performing nonlinear time history analysis with a sequence of mainshock and aftershock ground motions (Luco et al. 2004; Uma et al. 2011), investigating also the effects of the design approaches (Abdelnaby 2018), the seismic region, the earthquake intensity measure (Hosseinpour and Abdelnaby 2017), the number of stories (Raghunandan et al. 2015).

Table 1 reports the main parameters characterizing the case studies (structural typology, number of stories, location) and the aftershock fragility curves (intensity measure of the aftershock I_a, EDP), relating to different studies.

3 Seismic structural health monitoring of buildings: performance parameters

S^2HM systems for civil buildings generally measure accelerations at a certain number of stories. Measurements are then processed to extract performance parameters able to provide information about damage states. Recent S^2HM approaches extract instantaneous modal-based parameters from accelerations recorded during a seismic event (Aloisio et al. 2021; Ditommaso et al. 2012; Giordano et al. 2020; Limongelli and Çelebi 2019; Quqa et al. 2021), when the structures may experience large excursions in the nonlinear field. Ditommaso et al. (Ditommaso et al. 2021) used the Stockwell transform to monitor the modal curvature variation during seismic events. Quqa et al. used the modal assurance distribution to identify instantaneous nonlinear normal modes (Quqa et al. 2021). However, in general, these parameters can hardly be related to performance measures due to their strong dependency on the specific structure. Also, the same variation of modal parameters can correspond to several different damage types and damage states, with very different safety concerns. For example, a given variation of the first modal frequency may correspond to the settlement of a pillar, the formation of a plastic hinge at a critical section, or the cracking of non-structural elements.

As an alternative, the inter-story drift, obtained by double integration of story accelerations (Dolce et al. 2017), can be generally used as a seismic performance parameter. The advantage of inter-story drift is the possibility to define thresholds corresponding to specific limit states. For instance, American codes, such as FEMA-356 (FEMA 2000) and ASCE/SEI 41-13 (ASCE 2013) defined threshold values of the inter-story drifts corresponding to performance limit states, addressed to as "Immediate Occupancy", "Life

Table 1 Aftershock fragility curves parameters

Reference	Typology	N. of stories	Location	I_a	EDP
(Abdelnaby 2018)	RC frame structure	3	Japan	PGA (g)	Inter-story drift
(Hosseinpour and Abdelnaby 2017)	RC frame structure	3, 7, 12	Mississippi	PGA (g), Sa (g)	Inter-story drift
(Raghunandan et al. 2015)	RC frame structure	2, 4, 8, 12	California	Sd (in)	Inter-story drift
(Jeong et al. 2012)	RC frame structure	4, 8, 12	California	PGV (m/s)	Inter-story drift
(Uma et al. 2011)	RC frame structure	5	New Zealand and the US	Sa (g)	Inter-story drift
(Luco et al. 2004)	Steel frame structure	3	California	Sa (g)	Peak roof drift
(Li et al. 2014)	Steel frame structure	4	California	Sa (g)	Inter-story drift

Safety", "Collapse Prevention", and "Collapse" (Roohi and Hernandez 2020). On the other hand, the main drawback of inter-story drifts is related to the difficulty of their practical estimation through double integration of acceleration measurements. These measurements are usually affected by noise due to monitoring devices. This drawback may be particularly important when low-cost sensors with a considerable noise floor level are employed. Indeed, acceleration noise (modeled as white noise), after integration, takes the form of a Brownian motion whose variance increases linearly with time (Kaya and Safak 2019). Nevertheless, pre-processing operations, such as bandpass filtering, can be applied to reduce this effect (Dolce et al. 2017). Also, the inter-story drift can be calculated by integrating the contribution of each mode separately (Kaya and Safak 2015), reducing the estimation error.

Assuming the use of suitable pre-processing operations, which are not the main focus of this study, the inter-story drift is here considered as the seismic performance parameter to manage the seismic emergency of buildings. It is assumed that at least two accelerometers are deployed at consecutive levels: for example, where a soft story behavior can be experienced, or at the top and at the bottom of the building to evaluate an average inter-story drift along with the building height.

4 Value of information analysis

The topic discussed in the previous sections, i.e., mainshock and aftershock fragility functions and S^2HM outcomes, are incorporated in the framework of the VoI in the following.

The VoI is formulated in the context of the Bayesian decision theory (Raiffa and Schlaifer 1961) which deals with decision-making in uncertain environments and is grounded on the Bayesian interpretation of probability and the expected utility theory (Neumann and Morgenstern 1947). In the Bayesian framework, the probability $P(S)$ assigned to a state S is intended as the degree of belief that such state is true. The expected utility theory by von Neuman and Morgenstern instead relates to the behavior of a decision-maker which, if they behave rationally, should select the action which maximizes their expected utility, i.e., minimum expected costs (Verzobio et al. 2021). The availability of additional information on the state S can change the degree of belief that such state is true and, as a consequence, the probability assigned to it. Ultimately, the new information can modify the selection of the optimal action.

The VoI is obtained by comparing the expected costs of the actions chosen through two types of decision analysis, the Prior and Pre-Posterior decision analyses. Both decision analyses are carried out before the new information on the state of the building is collected. However, the Prior decision analysis is performed considering only the (prior) knowledge of the decision-maker, that is it does not consider the monitoring information. The Pre-Posterior decision analysis is performed accounting for the monitoring information ("Posterior" to the future acquisition of the information) but before the information is collected ("Pre" with respect to the actual acquisition of the information). The Pre-Posterior decision analysis requires thus the modeling of the future monitoring information.

A framework to compute the VoI for seismic emergency management of bridges was presented in (Giordano and Limongelli 2020). In the following subsections, this framework is described and adapted to the case of buildings.

4.1 Decision analyses

It is assumed that, after a mainshock, the building can be in one of the L discrete damage states DS_l, $l = 1, \ldots, L$, that cover the spectrum between no damage/minor damage up to severe damage. The decision-maker disposes of a set of decision alternatives constituted by several possible management actions A_n, $n = 1, \ldots, N$. "Evacuate" or "Do not evacuate" are two of such decision alternatives. The decision analysis aims at selecting the action corresponding to the minimum expected management cost.

In the ideal case in which the damage state of the building is known with certainty, the decision-maker can compute the expected cost of each action A_n, $E\left[c\left(A_n\right)|DS_l\right]$, which depends on DS_l. This expected cost can be computed considering the probability of failure of the building in DS_l and the direct and indirect costs associated with each action A_n. Assuming an aftershock as the possible cause of the failure, the expected cost of A_n is conditioned on the damage state DS_l of the building at the occurrence of the aftershock. Since the characteristics of the aftershock depend on those of the mainshock, the expected cost of A_n is also conditioned on the characteristics of the mainshock that will be represented through its magnitude M_m and epicentral distance R_m i.e., $E\left[c\left(A_n\right)|M_m, R_m, DS_l\right]$. This expected cost can be computed as follows:

$$E\left[c\left(A_n\right)|M_m, R_m, DS_l\right] = c_F\left(A_n\right)P\left(F\middle|M_m, R_m, DS_l\right) + c_{\overline{F}}\left(A_n\right)\left[1 - P\left(F\middle|M_m, R_m, DS_l\right)\right] \tag{3}$$

where $P\left(F\middle|M_m, R_m, DS_l\right)$ is the probability of failure due to aftershocks (see Sect. 4.4), $c_F\left(A_n\right)$ and $c_{\overline{F}}\left(A_n\right)$ are the cost of failure and survival, respectively, which depend on the action A_n.

The actual damage state of the building after a mainshock is usually unknown, thereby the decision-maker must consider all the possible damage states DS_l and corresponding probabilities of occurrence $P\left(DS_l|I_m\right)$, that are conditioned on I_m. The prior probabilities can be obtained from mainshock fragility curves (see Sect. 2.1) as follows:

$$\begin{cases} P\left(DS_l|I_m\right) = P\left(EDP \geq EDP_l|I_m\right) - P\left(EDP \geq EDP_{l+1}|I_m\right) & for\ l < L \\ P\left(DS_l|I_m\right) = P\left(EDP \geq EDP_l|I_m\right) & for\ l = L \end{cases} \tag{4}$$

where $EDP_1 = 0$. Considering all the possible damage states, the expected cost of the action can be computed using the total probability rule, as follows:

$$E[c\left(A_n\right)|\boldsymbol{\Theta}_\mathbf{m}] = \sum_{l=1}^{L} E[c\left(A_n\right)|M_m, R_m, DS_l]P(DS_l|I_m) \tag{5}$$

where the vector $\boldsymbol{\Theta}_\mathbf{m} = \left[M_m, R_m, I_m\right]$ contains the parameters that describe the mainshock. The optimal action $\hat{A}$ is chosen among all the possible decision alternatives A_n as the one corresponding to minimum expected costs $c_1\left(\boldsymbol{\Theta}_\mathbf{m}\right)$, as follows:

$$\hat{A} = \hat{A}\left(\boldsymbol{\Theta}_\mathbf{m}\right) = arg\min_n E\left[c\left(A_n\right)\middle|\boldsymbol{\Theta}_\mathbf{m}\right] \tag{6}$$

$$c_1\left(\boldsymbol{\Theta}_\mathbf{m}\right) = E\left[c\left(\hat{A}\right)|\boldsymbol{\Theta}_\mathbf{m}\right] = \sum_{l=1}^{L} E\left[c\left(\hat{A}\right)|M_m, R_m, DS_l\right]P\left(DS_l|I_m\right) \tag{7}$$

The suffix 1 in c_1 indicates that this expected cost is computed through a Prior decision analysis that is without the support of the monitoring information.

When one of the possible outcomes of an SHM system O_j, $j = 1, \ldots, J$ is available, the prior probabilities $P(DS_l|I_m)$ of the damage states can be updated based on this new knowledge. It should be noted that, in this study, we assume the identified inter-story drift as an observation of the SHM system (see Sect. 3). The updating of the prior probabilities is done through the Bayes' theorem, namely:

$$P\left(DS_l\middle|O_j, I_m\right) = \frac{P(O_j|DS_l)P(DS_l|I_m)}{P(O_j|I_m)} \tag{8}$$

where $P\left(DS_l\middle|O_j, I_m\right)$ is the probability of the damage state DS_l estimated accounting for the monitoring information. The term $P(O_j|DS_l)$ is the likelihood function, that is the probability of observing the outcome O_j when the building is in a damaged state DS_l. The denominator $P(O_j|I_m)$ represents the total probability (e.g., computed across all the possible damage states) of observing the monitoring outcome O_j when an earthquake of intensity measure I_m occurs:

$$P(O_j|I_m) = \sum_{l=1}^{L} P(O_j|DS_l)P(DS_l|I_m) \tag{9}$$

For each outcome O_j, the decision-maker selects the optimal action $\breve{A}_{O_j}$:

$$\breve{A}_{O_j} = \breve{A}(O_j, \boldsymbol{\Theta}_\mathbf{m}) = arg\ \min_n E\left[c\left(A_n\middle|O_j, \boldsymbol{\Theta}_\mathbf{m}\right)\right] \tag{10}$$

The corresponding minimum expected cost is:

$$E\left[c\left(\breve{A}_{O_j}\right)|O_j, \boldsymbol{\Theta}_\mathbf{m}\right] = \sum_{l=1}^{L} E[c\left(\breve{A}_{O_j}\right)|M_m, R_m, DS_l]P(DS_l|O_j, I_m) \tag{11}$$

According to Eq. 11, an optimal action corresponds to each outcome of the monitoring system. The Pre-Posterior decision analysis is carried out before the outcome is collected thereby the expected cost must be computed considering all the possible outcomes of the monitoring system, each weighted by its probability of occurrence for a given mainshock, $P(O_j|I_m)$. The cost $c_0(\boldsymbol{\Theta}_\mathbf{m})$ computed through the Pre-Posterior decision analysis (in this case, the suffix 0 is used) is given by:

$$c_0(\boldsymbol{\Theta}_\mathbf{m}) = \sum_{j=1}^{J} E\left[c\left(\breve{A}_{O_j}\right)|O_j, \boldsymbol{\Theta}_\mathbf{m}\right]P(O_j|I_m) \tag{12}$$

4.2 Value of information

The VoI for a mainshock defined by the vector $\boldsymbol{\Theta}_\mathbf{m}$ is computed as the difference between the Prior decision analysis cost, $c_1(\boldsymbol{\Theta}_\mathbf{m})$, and the Pre-Posterior cost $c_0(\boldsymbol{\Theta}_\mathbf{m})$, namely:

$$\mathrm{VoI}(\boldsymbol{\Theta}_\mathbf{m}) = c_1(\boldsymbol{\Theta}_\mathbf{m}) - c_0(\Theta_\mathbf{m}) \tag{13}$$

Equation 13 gives the VoI provided by the monitoring system if a mainshock $\mathbf{\Theta_m}$ occurs. However, since the VoI is computed when the monitoring system is installed, that is before the mainshock happens, the probability distributions of the parameters M_m, R_m and I_m (that characterize $\mathbf{\Theta_m}$) must be accounted for. The VoI is obtained as follows:

$$\mathrm{VoI} = \iiint_{M_m,R_m,I_m} \mathrm{VoI}(M_m,R_m,I_m) f(I_m|M_m,R_m) f(M_m) f(R_m)\, dI_m dM_m dR_m \tag{14}$$

where $f(I_m|M_m,R_m)$ is the Probability Density Function (PDF) of I_m conditioned on M_m and R_m, $f(M_m)$ and $f(R_m)$ are the PDFs of the magnitude and the epicentral distance, respectively.

The VoI computed utilizing Eq. 14 relates to a single seismic event. However, the estimation of the VoI must be performed to decide how much can be invested in a monitoring system that will provide information for a period T_{LC}. The VoI must thus be computed over the period T_{LC}, for which monitoring is envisaged. To this aim, the Life Cycle $\mathrm{VoI_{LC}}$ can be used (Zonta et al. 2014):

$$\mathrm{VoI_{LC}} = \sum_{i=1}^{T_{LC}} \lambda_m \frac{\mathrm{VoI}}{(r+1)^i} \tag{15}$$

where λ_m is the annual rate of earthquake occurrence and r is the discount rate. The $\mathrm{VoI_{LC}}$ can be interpreted as the expected reduction in emergency management costs in the period T_{LC}, provided by the SHM system.

4.3 Seismic hazard

In the previous sections, the seismic hazard was integrated into the definition of the VoI through the probability distributions of the parameters of the mainshock and the aftershock. The relevant models adopted herein are provided in the following.

As for mainshocks, a stationary Poisson model is adopted for their occurrence (Anagnos and Kiremidjian 1988). The PDF of the mainshock magnitude, $f(M_m)$, is modelled as truncated exponential function as follows:

$$f(M_m) = \frac{\beta e^{-\beta M_m}}{e^{-\beta M_{m,l}} - e^{-\beta M_{m,u}}} \tag{16}$$

where $M_{m,l}$ and $M_{m,u}$ are the lower and upper bounds, respectively, of the mainshock magnitude, and $\beta = b \ln 10$, where b is the Negative slope of the Gutenberg-Richter law. An area source model (Baker 2013) is used in which the earthquakes are generated with uniform probability inside the seismogenic area whose geometric properties determine the distribution of the source-to-site distances. The distribution of the intensity measure conditioned on the magnitude and the distance of the earthquake $f(I_m|M_m,R_m)$ is determined using Ground Motion Prediction Equations (GMPEs) available in the literature (Douglas 2011). GMPEs allow accounting for the uncertainty in the physical parameters of fault rupture which have a strong influence on the uncertainties of structural conditions.

As for aftershocks, they are modeled as a nonhomogeneous Poisson process in which their occurrence rate decreases with increasing elapsed time after the mainshock. The magnitudes of the aftershocks are assumed to be bounded between a lower and an upper bound. The lower bound is taken equal to the lower bound of mainshock magnitudes whereas the upper bound

is taken equal to the magnitude of the mainshock which caused the aftershocks. The mean number of aftershocks in the period $[t;t+T]$, following a mainshock of magnitude M_m, reads:

$$N_a\left(M_m,t,T\right)=\frac{10^{a+b\left(M_m-M_{m,l}\right)}-10^{a}}{p-1}\left[(c+t)^{1-p}-(c+t+T)^{1-p}\right] \tag{17}$$

where a, b, c, and p are parameters that depend on the seismic area and $M_{m,l}$ is the lower bound of aftershock magnitudes.

The PDF of the aftershock magnitude depends on the magnitude of the mainshock, and it is expressed as follows:

$$f\left(M_a\middle|M_m\right)=\frac{\beta e^{-\beta\left(M_a-M_{m,l}\right)}}{1-e^{-\beta\left(M_m-M_{m,l}\right)}} \tag{18}$$

where $\beta=b\ln 10$.

It is assumed that aftershocks occur with uniform probability in a circular region centered at the mainshock location. The area of this region is expressed as a function of M_m (Utsu 1970), as follows:

$$S_a=10^{M_m-4.1} \tag{19}$$

Hence, the distribution of source-to-site distances for aftershock $f\left(R_a\middle|M_m,R_m\right)$ is conditioned on both M_m and R_m.

The GMPE used for mainshocks is also used for aftershocks, providing $f\left(I_a\middle|M_a,R_a\right)$. The PDF of I_a can be conditioned on M_m and R_m as follows:

$$f\left(I_a\middle|M_m,R_m\right)=\iint\limits_{M_a,R_a} f\left(I_a\middle|M_a,R_a\right)f\left(M_a\middle|M_m\right)f\left(R_a\middle|M_m,R_m\right)dM_a dR_a \tag{20}$$

4.4 Probability of failure

The probability of failure due to aftershocks depends on the conditions of the building after the mainshock and the characteristics of the aftershocks, which in turn depend on those of the mainshock, i.e., $P\left(F\middle|M_m,R_m,DS_l\right)$. First, the probability of failure due to a single aftershock, $P^*\left(F\middle|M_m,R_m,DS_l\right)$, must be evaluated, which reads:

$$P^*\left(F\middle|M_m,R_m,DS_l\right)=\int\limits_{I_a} P\left(F\middle|I_a,DS_l\right)f\left(I_a\middle|M_m,R_m\right)dI_a \tag{21}$$

where $P\left(F\middle|I_a,DS_l\right)$ is the aftershock fragility function (see Sect. 2.2) and the term $f\left(I_a\middle|M_m,R_m\right)$ is obtained using Eq. 20. The probability of failure due to a single aftershock is then employed to obtain the mean number of aftershocks $N_F\left(M_m,R_m,DS_l,t,T\right)$ that induce the failure of the structure in the time interval $[t;t+T]$, as follows:

$$N_F\left(M_m,R_m,DS_l,t,T\right)=P^*\left(F\middle|M_m,R_m,DS_l\right)N_a\left(M_m,t,T\right) \tag{22}$$

where $N_a\left(M_m,t,T\right)$ is the mean number of aftershocks in the period $[t;t+T]$ defined by Eq. 17 Finally, the probability of failure in the period $[t;t+T]$ is obtained as:

$$P\left(F\middle|M_m, R_m, DS_l\right) = 1 - e^{-N_F\left(M_m, R_m DS_l, t, T\right)} \tag{23}$$

5 Application

The theoretical framework of the VoI described in the previous sections is applied to an exemplary case study introduced to investigate the effect of different parameters on the VoI. The following decision problem is considered. The manager of a building in a seismic-prone area is considering the adoption of an S^2HM system to support the management of the emergency phase following an earthquake. After the mainshock, the building could be damaged, and the decision-maker must select the optimal action between "Evacuate" and "Do not evacuate" the building. The decision-maker must consider the costs of the two decision alternatives. The evacuation of the building after the mainshock involves indirect losses, due for instance to business interruption and reallocation costs. On the other hand, if the building is not evacuated, it might fail due to aftershocks and cause fatalities. When the S^2HM information is not available, decision-making is performed based on prior knowledge (i.e., fragility curves and GMPE). The S^2HM system provides information on the structural state, thus reducing the uncertainty that affects the decision problem. A sensitivity analysis with respect to several parameters characterizing the case study is performed to demonstrate how they affect the VoI.

5.1 Description of the case study

5.1.1 Fragility model

Three building models are considered in this study. They were originally developed in (Raghunandan 2012; Raghunandan et al. 2015). The buildings consist of different RC moment frame structures of varying height and number of floors designed according to the modern US seismic design regulations. The main properties of these buildings are displayed in Table 2. The rationale behind the selection of these case studies relates to the availability of the parameters of mainshock and aftershock fragility functions for different levels of damage, defined in terms of maximum Inter-Story Drift (ISD) ratio.

It is assumed that, after the mainshock, the structures can be in one of the three discrete damage states DS_l, defined as follows: DS_1 for $ISD < 0.020$, DS_2 for $0.020 \leq ISD < 0.040$, DS_3 for $ISD \geq 0.040$. The parameters that describe the mainshock and aftershock fragility functions, i.e., median capacities and lognormal standard deviations (see Sects. 2.1., 2.2.) are displayed in Table 3. The inelastic spectral displacement S_{di} is the intensity measure adopted to describe the ground motion intensity, which is the peak displacement of a

Table 2 Information on the buildings

	2 floors	8 floors	12 floors
Fundamental period, T_1 [s]	0.60	1.81	2.15
Yield displacement, u_y [m]	0.046	0.122	0.145
C_y [m/s^2]	5.039	1.469	1.237

Table 3 Parameters of mainshock and aftershock fragility curves (from (Raghunandan 2012))

		Median capacity [in m] and associated β_{tot} (in brackets)		
		2 floors	8 floors	12 floors
Mainshock	I_{DS_2}	0.15 (0.21)	0.26 (0.17)	0.32 (0.21)
	I_{DS_3}	0.21 (0.23)	0.43 (0.21)	0.52 (0.20)
Aftershock	$I_{F(DS_1)}$	0.26 (0.26)	0.57 (0.25)	0.62 (0.24)
	$I_{F(DS_2)}$	0.22 (0.26)	0.47 (0.28)	0.48 (0.31)
	$I_{F(DS_3)}$	0.17 (0.35)	0.38 (0.34)	0.33 (0.38)

bilinear SDOF oscillator when subjected to the ground motion of interest (Tothong and Luco 2007).

The probabilities of failure due to aftershocks are computed as functions of M_m and R_m for each threshold, defined in terms of ISD. In turn, the probability of failure for the damage states—each delimited by two thresholds—is computed as the mean value of the probabilities of failure relevant to the two thresholds.

5.1.2 Hazard model

It is assumed that the buildings are in the center of the circular seismogenic area shown in Fig. 2 which produces earthquakes randomly and with equal probability in any location.

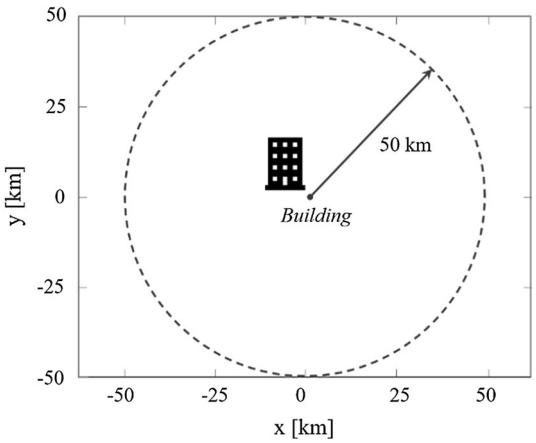

Fig. 2 Location of the building and seismogenic area

Table 4 Parameters defining mainshocks and aftershocks

Mainshock		Aftershock	
Variable	Value	Variable	Value
Minimum magnitude,$M_{m,l}$	5	a	− 1.67
Maximum magnitude,$M_{m,u}$	From 7 to 9	b	0.91
Negative slope of the Gutenberg–Richter relation,b	1	c	0.05
		p	1.08

The parameters defining the mainshocks and aftershocks are reported in Table 4. In particular, the aftershock parameters are selected for a generic aftershock sequence in California (Reasenberg and Jones, 1989).

The inelastic spectral displacement S_{di}, used as intensity measure in the fragilities previously described, can be expressed as a function of the ductility demand μ and the elastic displacement u_y specifically, $S_{di} = u_y\mu$. In turn, the ductility demand μ due to earthquakes is obtained using the GMPE proposed in (Rupakhety and Sigbjörnsson 2009) in the form:

$$\log_{10}(\mu) = b_1 + b_2 M_w + b_3 \log_{10}\sqrt{d^2 + b_4^2} + b_5 S + \varepsilon \tag{24}$$

where b_1, b_2, b_3, b_4, and b_5 are regression coefficients [tabulated in (Rupakhety and Sigbjörnsson 2009)] depending on the undamped natural period T, the critical damping ratio ξ, and mass normalized yield strength $C_y = u_y(2\pi/T)^2$, S is a parameter depending on the soil type (assumed equal to 1), and ε is a zero mean normal random variable with standard deviation σ_ε.

5.1.3 Information model

The S^{2}HM outcome employed in this study is the maximum *ISD* ratio measured during the strong motion. For simplicity of notation, in the following, the maximum *ISD* ratio is indicated simply as *ISD*. It must be considered that: (1) by definition of the damage states DS_l, a range of *ISD* values corresponds to each of them, and (2) the observed values of *ISD* are affected by uncertainty.

To simplify the information modeling, it is herein assumed that K values of ISD_k ($k = 1, 2, \ldots K$) correspond to each damage state DS_l. The probability that the S^{2}HM provides an outcome O_j, when the structure is in damage state DS_l can be expressed as follows:

$$P(O_j|DS_l) = \sum_{k=1}^{K} P(O_j|ISD_k)P(ISD_k|DS_l) \tag{25}$$

where $P(O_j|ISD_k)$ is the probability to observe O_j when the real value of the *ISD* is ISD_k and $P(ISD_k|DS_l)$ is the probability that ISD_k occurs when the structure is in the damage state DS_l.

It is mentioned that the inter-story drift and its observations are continuous variables and therefore the integral version of Eq. 25 should be considered. Herein it is assumed that the values *ISD* are uniformly distributed within each damage state, see Fig. 3. For instance, for DS_2, each of the values of *ISD* in the range $0.02 - 0.04$ has the same value of PDF, equal to $1/(0.04 - 0.02) = 50$.

The distribution of the observation of a given value of the inter-story drift*aa* is modeled through a Normal distribution with mean equal to the "real" value of the inter-story drift *ISD* and standard deviation $\sigma = 0.05 \cdot ISD$.

The probability distributions of the S^{2}HM outcomes in the three damage states are reported in Fig. 4.

The proportionality assumed for σ and *ISD* implies that the uncertainty in the value of the S^{2}HM observation increases with damage. The rationale behind this assumption is that the error in the identified parameters generally grows with the structural nonlinearities (Shan et al. 2015), which are typically amplified by damage (Kerschen et al. 2006).

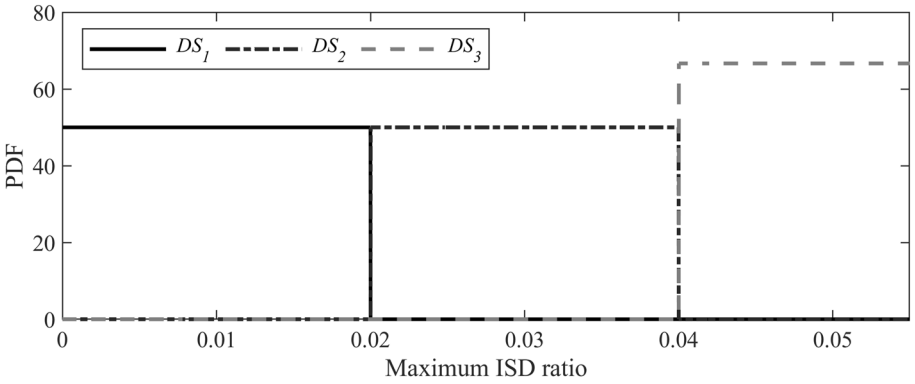

Fig. 3 Distribution of the ISD ratio in the three damage states

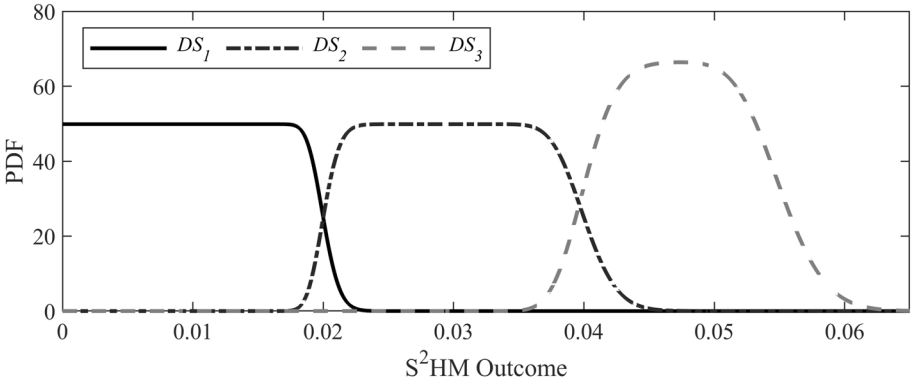

Fig. 4 Distribution of the S^2HM outcome in the three damage states

Most identification methods are indeed based on the assumption of structural linear behavior. Thus, they accumulate inaccuracies as the structure undergoes damage. While in the case of linear structures, the numerical integration method has shown to accumulate within 1–4% error at peak displacement prediction (Skolnik and Wallace 2010), structures undergoing inelastic deformations, generally accumulate considerable residual displacement (Shan et al. 2015).

5.1.4 Costs

As for the costs involved in the decision analysis, it is supposed that the number of people per floor, N_{pf} [person/floor], is 20. The number of floors is indicated as N_f. The duration of the emergency is indicated as T [day]. The reference cost of each fatality, F[$/person], is approximated to 2 million dollars (Wong et al. 2005). This cost should be intended as the statistical value of generic human life, used for instance by an insurance company for recompensing purposes. Initially, it is assumed that:

Table 5 Cost of failure and survival

	$A_n = Evacuate$	$A_n = Do\ not\ evacuate$
$c_F(A_n)$ [$]	$IC = TN_f C$	$DC = FN_f N_{pf}$
$c_{\overline{F}}(A_n)$ [$]	$IC = TN_f C$	0

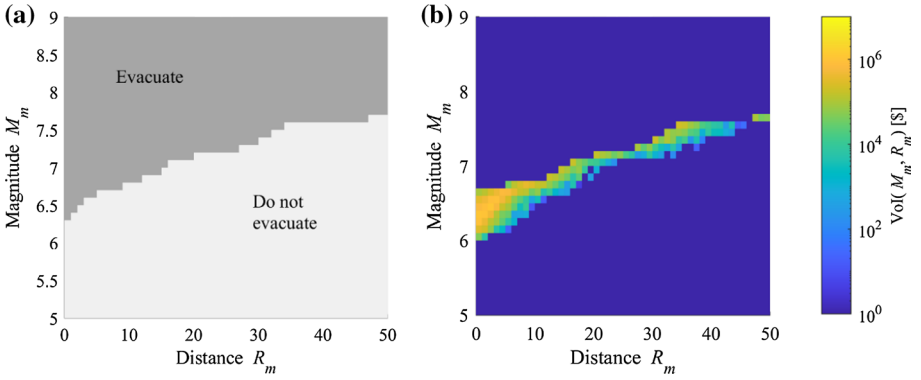

Fig. 5 Results for $M_{m,u} = 9$ and C = 5,000 $: **a** Optimal action according to the Prior decision analysis; **b** $\mathrm{VoI}(R_m, M_m)$

- If the building is not evacuated and fails because of an aftershock, all the people in the building die.
- If the building is not evacuated and it does not fail, it is assumed that there are no costs to pay.
- If the building is evacuated, there are indirect costs that do not depend on the state of the building. These costs are defined by the daily indirect cost per floor C [$/floor/day].

The costs of failure, $c_F(A_n)$, and survival, $c_{\overline{F}}(A_n)$, as a function of the selected action (see Eq. 3) are displayed in Table 5. The cost of the action "Evacuate" is indicated as $IC = TN_f C$ (Indirect Cost) whereas $DC = FN_f N_{pf}$ (Direct Cost) indicates the cost associated with failure when the structure is not evacuated.

5.2 Results

The VoI analysis is carried out to investigate the impact of the seismicity of the region, the magnitude of the indirect costs, the emergency duration, the prior knowledge, and the indirect costs related to the failure. The results are presented and discussed in the following sections.

5.2.1 Variation of VoI with the seismicity of the region

First, three cases corresponding to different hazard levels are described considering different values of the indirect costs. They are all relevant to a 12-story building and a reference period $T = 60 days$.

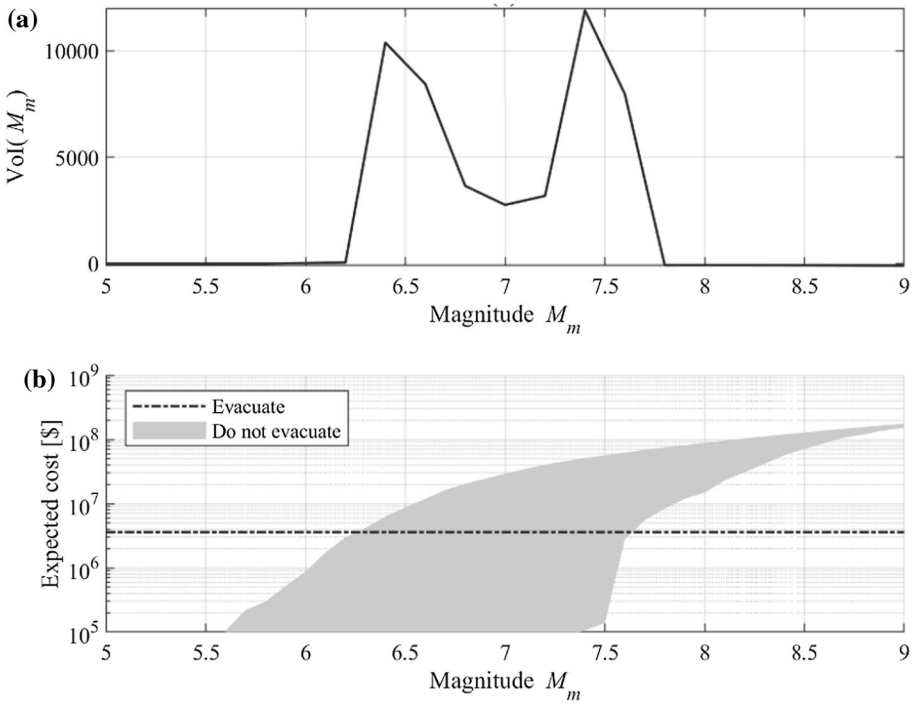

Fig. 6 Results for $M_{m,u} = 9$ and C = 5000 $: **a** VoI$(M_m)$ and **b** prior expected costs

Figures 5 and 6 report the results relevant to Case 1: high seismicity region $(M_{m,u} = 9)$ and low indirect costs $(C = 5000\$)$. Figure 5a illustrates the outcome of the Prior decision analysis (that is performed without the support of the S^2HM information) in terms of the optimal action chosen as a function of M_m and R_m. As expected, the action "Do not evacuate" is preferable for mainshocks of low magnitude with an epicenter far from the building (low right end corner of the figure) whereas the optimal action is "Evacuate" when high magnitude earthquakes occur close to the building (upper left corner of the figure). The boundary between the two optimal actions corresponds to earthquakes (e.g., combinations of M_m and R_m) for which the expected costs of the two actions are very close to each other. This boundary moves toward higher values of M_m at the increase of the epicentral distance R_m. The VoI, reported in Fig. 5b reaches the maximum values in a narrow region around this boundary. Indeed, where the two management actions have similar expected costs, the information from the S^2HM system provides the highest benefit. This aspect is highlighted in Fig. 6, which report the VoI (Fig. 6a) and the expected costs of the two emergency management actions (Fig. 6b) as a function of the event magnitude M_m. The grey region in Fig. 6b indicates, for each value of the magnitude M_m, the expected cost relevant to different values of the epicentral distance R_m in the range (0–50 km). The upper and lower boundaries of the grey region correspond respectively to $R_m = 0km$ (maximum probability of failure and therefore maximum expected cost for a given magnitude) and $R_m = 50km$ (minimum probability of failure and therefore minimum expected cost for a given magnitude). The dash-dotted line represents the—constant in this case—expected cost of the action "Evacuate". The

maximum VoI is located in the magnitude range 6.5–7.5, roughly, corresponding to the intersection between the dash-dotted line and the grey region: here the two decision alternatives lead to equal prior expected costs.

Figure 7 shows the results obtained for Case 2: high seismic hazard and high indirect costs: $C = 50,000\$$. In this case, the action "Evacuate" becomes optimal in a range of higher magnitudes with respect to Case 1 (Figs. 6a, 7a). This is due to the higher values of C with respect to Case 1, which leads to higher indirect costs related to the action "Evacuate". On the other hand, the expected cost of the action "Do not evacuate" is the same as Case 1 since it mainly depends on the probability of failure and thereby on the seismicity of the region. Graphically, the dashed-dot horizontal line moves up and crosses the curves corresponding to the direct costs (grey region) in the range of higher magnitudes, around 8–9. In this same region, the VoI reaches its maximum values Fig. 7a and presents higher values with respect to Case 1. This is due to the higher expected costs of the two management actions that lead to a higher value of their difference representing the benefit achieved when the decision-maker changes her decision thanks to the S^2HM information.

Figure 8 shows the VoI as a function of M_m (Fig. 8a), computed by marginalizing out the term R_m from $\mathrm{VoI}(R_m, M_m)$, and the expected costs of the two actions (Fig. 8b). The VoI is again maximum where the expected costs of the two actions are similar which, in this case, happens in the magnitude range 7.5–8.5. It is underlined that Figs. 6b and 8b differ in the position of the horizontal line represented by the (fixed) expected cost of the action "Evacuate" whereas the grey region corresponding to the expected cost of the action "Do not evacuate" is the same (the same direct costs are considered).

Case 3 is relevant to a region at medium seismic hazard $(M_{m,u} = 8)$ and high indirect costs $(C = 50,000\$)$. The meaning of the figures is the same as for the previous cases. Figure 9 shows that the optimal action identified based on Prior decision analysis is "Evacuate" only for a small area on the upper left corner of the plot, due to the lower direct costs with respect to Case 2. Consequently, significative values of the VoI are reached only for high values of magnitude.

Figure 10 shows the VoI as a function of M_m (Fig. 10a) and the prior expected costs of the two actions (Fig. 10b). The prior expected costs of the action "Do not evacuate" (direct costs) are generally lower with respect to Case 2 due to lower seismic demand, leading to a lower probability of failure. Figure 10a shows that the VoI monotonically increases

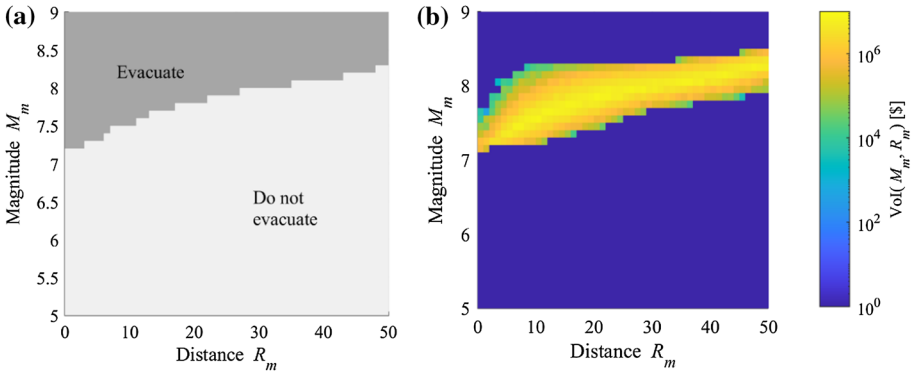

Fig. 7 Results for $M_{m,u} = 9$ and C = 50,000 $: **a** Optimal action according to the Prior decision analysis, and **b** $\mathrm{VoI}(R_m, M_m)$

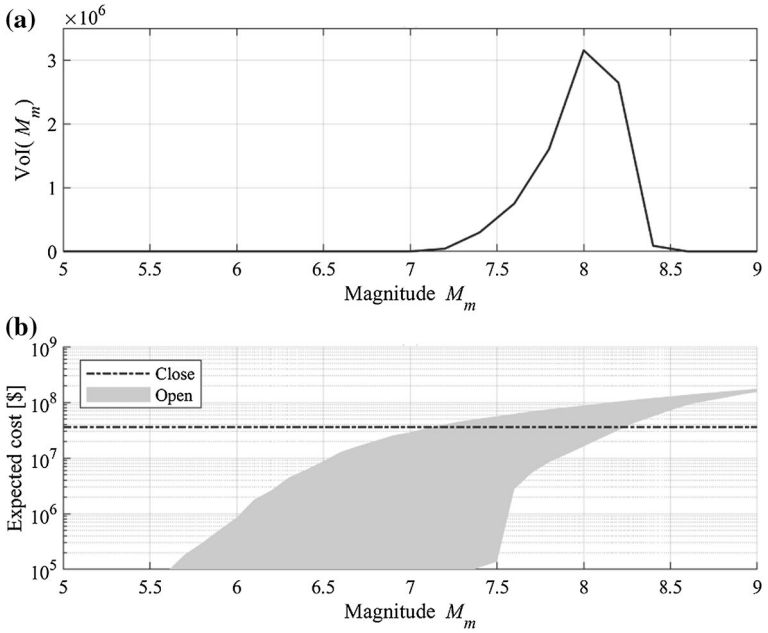

Fig. 8 Results for $M_{m,u} = 9$ and C = 50,000 $: **a** $\mathrm{VoI}(M_m)$ and **b** prior expected costs

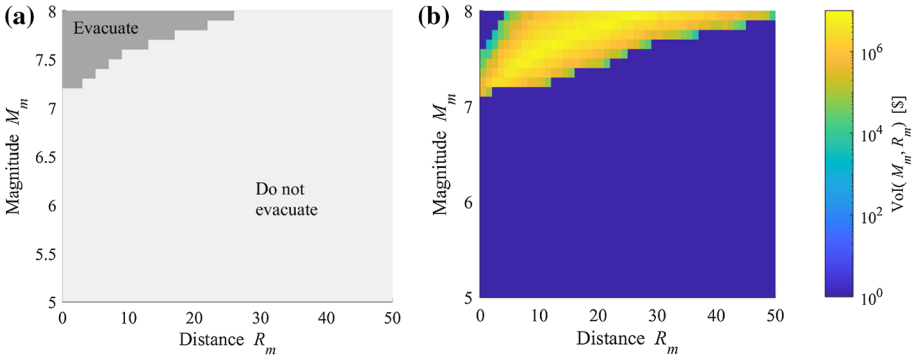

Fig. 9 Results for $M_{m,u} = 8$, C = 50,000 $, and $N_f = 12$: **a** Optimal action according to the Prior decision analysis, and **b** $\mathrm{VoI}(R_m, M_m)$

over the range of magnitudes since there is no range of magnitude in which the expected cost of the action "Do not evacuate" is always higher than the expected cost of the action "Evacuate".

5.2.2 Variation of VoI with the indirect costs

To investigate the impact of the daily indirect costs C on the VoI, the analysis is repeated for several different values of this parameter and the results are displayed in Fig. 11. The analysis is carried out considering buildings of a different number of floors in different

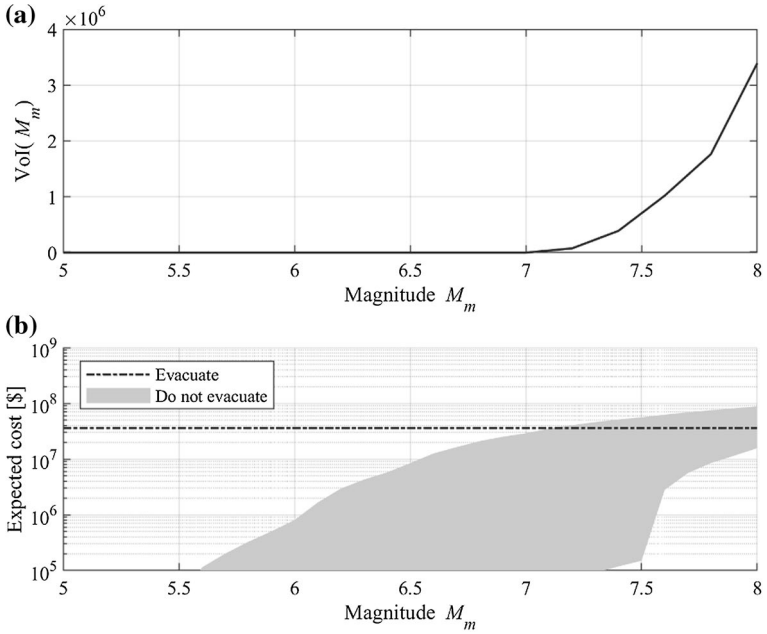

Fig. 10 Results for $M_{m,u} = 8$, C = 50,000 $, and $N_f = 12$: **a** $\mathrm{VoI}(M_m)$ and **b** prior expected costs

seismogenic areas. Specifically, three different upper bound for magnitudes $M_{m,u}$ have been considered, from 7 to 9 (see Sect. 4.3 and Table 4). The duration of the emergency duration is fixed to $T = 60 days$. Different values of C represent different intended uses of the buildings. For instance, low values of C can be associated with residential use when indirect losses are related to the cost of alternative accommodations such as hotels. Instead, high values of C can be associated with cases where a business interruption may have a higher cost.

Results show that, for the same building, the VoI increases with the seismicity of the area, that is for increasing values of $M_{m,u}$. Furthermore, the VoI increases with the number of floors. Specifically, increasing values of $M_{m,u}$ imply the increase of the seismic exposure of the buildings meaning higher probabilities of failure (for a given couple M_m and R_m) and probabilities of occurrence of earthquakes with high magnitudes. The increasing number of floors, instead, involves the increase of both direct and indirect costs. It is highlighted that the VoI is negligible for very low or very high values of C, which is when the indirect costs are very low or very high. In this situation, the prior expected costs of the two decision alternatives ("Evacuate" or "Do not evacuate") are very different and, as found in other studies (Giordano et al. 2020; Giordano and Limongelli 2020), this leads to negligible values of the VoI. The reason is that in this situation, the information from the S^2HM does not change the behavior of the decision-maker. For low values of C (low indirect costs) the action "Evacuate" appears very convenient; for high values of C (high indirect costs) the action "Evacuate" is very expensive and therefore "Do not Evacuate" becomes the optimal action, regardless of the state of the system. If the state of the system does not affect the decision, its knowledge and thereby the information from the S^2HM, becomes irrelevant. To improve clarity, a second horizontal axis has been included in the three plots in Fig. 11 showing the values of the ratio IC/DC that correspond to each C. For values of

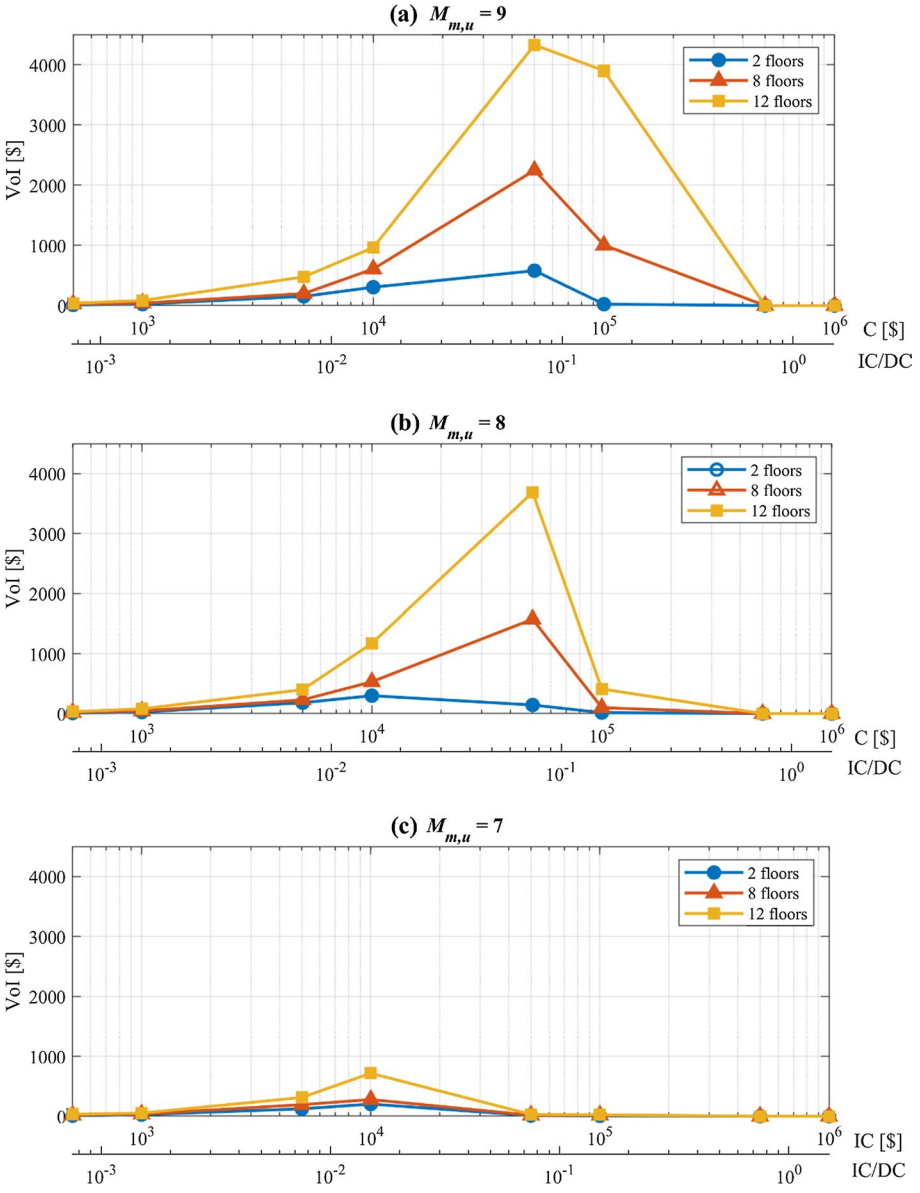

Fig. 11 **a** VoI for $M_{m,u} = 9$, **b** $M_{m,u} = 8$, and **c** $M_{m,u} = 7$

$IC/DC > 1$ the VoI is null since the action "Do not evacuate" is always the optimal action independently of the state of the system. For IC/DC close to zero the indirect costs are much lower with respect to the direct costs and so the action evacuate is the optimal, irrespective of the building state.

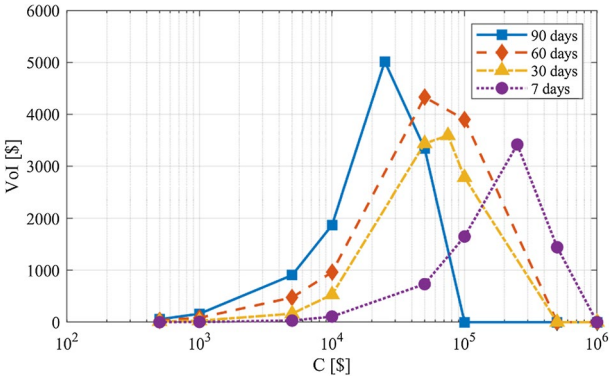

Fig. 12 VoI as a function of C and duration of the emergency T for $M_{m,u} = 8$ and $N_f = 12$

5.2.3 Variation of VoI with the emergency duration

Figure 12 shows the results for different values of T, i.e., the duration of the emergency period. The increase of T leads to the increase of the indirect costs that depend linearly on T (see Table 5), and of the direct costs, due to the increase of the probability of failure (see Sects. 4.3., 4.4.). Results indicate that the VoI increases with the increasing duration of the emergency period since both direct and indirect costs increase. Furthermore, the peak of the VoI moves towards lower values of C which indicates that the indirect costs increase more rapidly with C with respect to the direct costs. However, the maximum VoI does not change significantly at the increase of the reference emergency period from 30 to 90 days.

5.2.4 Variation of VoI with the prior knowledge

In the previous sections, the VoI provided by the S^2HM was computed assuming that the decision-maker disposes of (aftershock) fragility curves as a support to manage the emergency. The information provided by the S^2HM enables the improvement of the knowledge on the system with respect to that provided by the fragility curves. However, the knowledge of the aftershock fragility curves is not always available, as shown by the literature survey reported

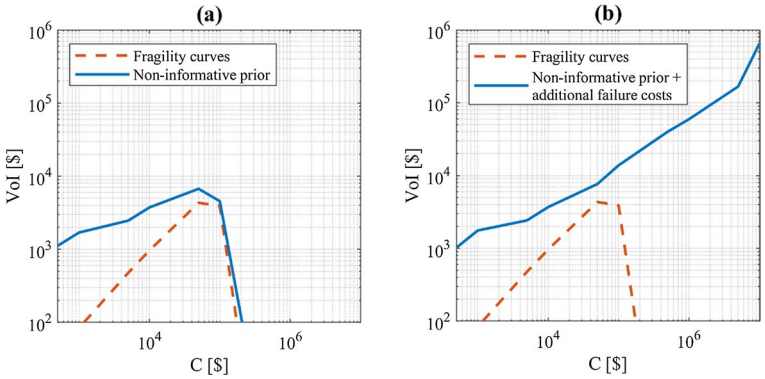

Fig. 13 VoI as a function of C: **a** effect of non-informative prior probabilities and **b** combined effect of non-informative prior probabilities and additional failure costs

in Sect. 2.2. To investigate the impact of the prior knowledge provided by the fragility curves, in this section, the VoI is computed attributing the same prior probability to each damage state $P(DS_1) = P(DS_2) = P(DS_3) = 1/3$ (non-informative prior probabilities). Figure 13a shows the VoI as a function of the daily indirect costs C obtained considering prior probabilities from fragility functions and non-informative prior probabilities. The analysis parameters are $T = 60\ days$, $M_{m,u} = 9$, and $N_f = 12$. The VoI relating to the case when fragility functions are available (red dashed line) is the same shown in Fig. 11a and is reported for comparison purposes. The VoI obtained considering non-informative prior probabilities is represented by the blue solid line and, for a given C, is generally higher than the VoI obtained considering prior probabilities from fragility curves. The use of the fragility functions is a way to include information in the decision-making process. Therefore, if this information is not included in the analysis, the knowledge acquired by means of the S^{2}HM system provides a higher benefit.

5.2.5 Variation of VoI with indirect costs associated with failure

In the previous sections, it has been assumed that the action "Do not evacuate" involves direct costs related to the fatalities but not indirect costs. However, in this situation, the collapse of the building entails not only the loss of the building itself but also of resources (human and material) needed for business continuity. To account for this aspect, in this section, an additional cost is introduced through a downtime period T^* intended as the time required to re-organize and re-allocate the activity carried out in the building. The relevant indirect costs are expressed as $T^* N_f C$; in the analysis the value $T^* = 365 days$ has been considered for demonstration.

Figure 13b displays the VoI computed considering non-informative prior probabilities and additional indirect costs associated with the structural failure, according to Table 6, considering the following parameters: $T = 60 days$, $M_{m,u} = 9$, and $N_f = 12$.

The VoI continuously increases with the indirect costs (represented by the daily indirect costs C). In this case, the VoI is not null for high values of the daily indirect costs. The reason is that the daily indirect costs affect the expected costs of both actions and thereby "Do not Evacuate" is not necessarilty the optimal action for high values of C (see Sect. 5.2.2). This result further confirms that the VoI strongly depends on the magnitude of the costs involved in the decision analysis and the difference between the expected costs of the management actions.

6 Conclusion

In this paper, the benefit of installing a permanent S^{2}HM on buildings to support emergency management is explored. To estimate this benefit, a framework based on the Value of Information (VoI) from Bayesian decision analysis is proposed and applied to reference case studies consisting of RC buildings with a different number of floors.

Table 6 Modified cost of failure and survival

	$A_n = Evacuate$	$A_n = Do\ not\ evacuate$
$c_F(A_n)$ [\$]	$TN_f C$	$FN_f N_{pf} + T^* N_f C$
$c_{\overline{F}}(A_n)$ [\$]	$TN_f C$	0

The computation of the VoI in this context has been carried out considering the availability: of (1) the seismic hazard model of the region where the building is located; (2) fragility curves that give insights into the structural conditions without SHM information; (3) likelihood functions to model the outcome of the S^2HM system in different system states; (4) consequences of failure and survival for different management actions.

A sensitivity analysis is carried out concerning: (1) the height of the building; (2) the seismicity of the region; (3) the ratio between indirect and direct consequences; (4) the duration of the emergency, which is defined as the interval between the mainshock, and the inspection performed by an expert technician; (5) the prior knowledge; (6) the indirect losses related to the failure of the building. Results show that:

- the VoI increases with the seismicity of the region and the number of building floors. Both factors are related to the expected costs of different actions. The higher the seismicity, the greater the probability of failure and the probability of being in a severe damage state. Thus, the expected cost of the action "Do not Evacuate" increases. A higher number of floors, instead, involves the increase of both direct and indirect costs and thus of the expected costs of both the action "Do not Evacuate" and the action "Evacuate".
- higher values of the VoI are obtained when different management actions have similar prior expected costs. In these cases, the optimal action is more uncertain and the information from the monitoring system strongly impacts the decision-making.
- the VoI is negligible when the prior expected costs of different management actions are very different from each other since the information from the S^2HM system does not modify the behavior of the decision-makers.
- the ratio between indirect and direct costs is the parameter that mostly influences the value of the VoI.

Acknowledgements Pier Francesco Giordano and Maria Pina Limongelli were partially funded by the Italian Civil Protection Department within the WP6 "Structural Health Monitoring and Satellite Data" 2019-21 ReLUIS Project.

Funding Funding is provided by Dipartimento della Protezione Civile, Presidenza del Consiglio dei Ministri (Grant No. WP6 "Structural Health Monitoring and Satellite Data" 2019-21 ReLUIS). Open access funding provided by Politecnico di Milano within the CRUI-CARE Agreement.

Declarations

Conflict of interest The authors declare that they have no conflict of interest.

References

Abdelnaby AE (2018) Fragility curves for RC frames Subjected to Tohoku mainshock-aftershocks sequences. J Earthq Eng 22:902–920. https://doi.org/10.1080/13632469.2016.1264328

Aloisio A, Antonacci E, Fragiacomo M, Alaggio R (2021) The recorded seismic response of the santa maria di collemaggio basilica to low-intensity earthquakes. IntJ Arch Herit 15(1):229–247. https://doi.org/10.1080/15583058.2020.1802533

Anagnos T, Kiremidjian AS (1988) A review of earthquake occurrence models for seismic hazard analysis. Probab Eng Mech 3:3–11. https://doi.org/10.1016/0266-8920(88)90002-1

ASCE (2013) Seismic evaluation and retrofit of existing buildings. Reston

Baker JW (2013) Probabilistic seismic hazard analysis. White Paper Version 2.0.1

Benjamin JR, Cornell CA (1970) Probability, statistics, and decision for civil engineers. McGraw-Hill

Bursi OS, Zonta D, Debiasi E, Trapani D (2018) Structural health monitoring for seismic protection of structure and infrastructure systems. In: Recent advances in earthquake engineering in Europe—16th European conference on earthquake engineering, Thessaloniki, pp 339–358

Cardone D, Flora A, De Luca PM, Martoccia A (2019) Estimating direct and indirect losses due to earthquake damage in residential RC buildings. Soil Dyn Earthq Eng 126:105801. https://doi.org/10.1016/j.soildyn.2019.105801

Ditommaso R, Mucciarelli M, Ponzo FC (2012) Analysis of non-stationary structural systems by using a band-variable filter. Bull Earthq Eng 10:895–911. https://doi.org/10.1007/s10518-012-9338-y

Ditommaso R, Iacovino C, Auletta G et al (2021) Damage detection and localization on real structures subjected to strong motion earthquakes using the curvature evolution method: the Navelli (Italy) case Study. Appl Sci 11:6496. https://doi.org/10.3390/app11146496

Dolce M, Nicoletti M, De Sortis A et al (2017) Osservatorio sismico delle strutture: the Italian structural seismic monitoring network. Bull Earthq Eng 15:621–641. https://doi.org/10.1007/s10518-015-9738-x

Douglas J (2011) Ground-motion prediction equations 1964–2010. Pacific Earthquake Engineering Research Center PEER 2011/102

FEMA (2000) Commentary for the seismic rehabilitation of buildings. Washington, DC

FEMA-NIBS (2012) Earthquake loss estimation methodology - HAZUS technical manual

Giordano PF, Limongelli MP (2020) The value of structural health monitoring in seismic emergency management of bridges. Struct Infrastruct Eng. https://doi.org/10.1080/15732479.2020.1862251

Giordano PF, Prendergast LJ, Limongelli MP (2020) A framework for assessing the value of information for health monitoring of scoured bridges. J Civ Struct Health Monit 10:485–496. https://doi.org/10.1007/s13349-020-00398-0

Giordano PF, Ubertini F, Cavalagli N, Kita A, Masciotta MG (2020) Four years of structural health monitoring of the san pietro bell tower in Perugia, Italy: two years before the earthquake versus two years after. Int J Mason Res Innov 5(4):445–467. https://doi.org/10.1504/IJMRI.2020.111797

Han R, Li Y, van de Lindt J (2016) Seismic loss estimation with consideration of aftershock hazard and post-quake decisions. ASCE-ASME J Risk Uncertaint Eng Syst Part A Civ Eng 2:04016005. https://doi.org/10.1061/AJRUA6.0000875

Hatzigeorgiou GD, Beskos DE (2009) Inelastic displacement ratios for SDOF structures subjected to repeated earthquakes. Eng Struct 31:2744–2755. https://doi.org/10.1016/j.engstruct.2009.07.002

Hosseinpour F, Abdelnaby AE (2017) Fragility curves for RC frames under multiple earthquakes. Soil Dyn Earthq Eng 98:222–234. https://doi.org/10.1016/j.soildyn.2017.04.013

Iacovino C, Ditommaso R, Ponzo FC, Limongelli MP (2018) The Interpolation evolution method for damage localization in structures under seismic excitation. Earthq Eng Struct Dyn 47:2117–2136. https://doi.org/10.1002/eqe.3062

Iacovino C, Flora A, Cardone D, Vona M (2021) Seismic assessment of masonry buildings at territorial scale. In: Compdyn 2021 and 8th ECCOMAS thematic conference on computational methods in structural dynamics and earthquake engineering

Iannacone L, Giordano PF, Gardoni P, Limongelli MP (2021) Quantifying the value of information from inspecting and monitoring engineering systems subject to gradual and shock deterioration. Struct Health Monit. https://doi.org/10.1177/1475921720981869

Jeong S-H, Mwafy AM, Elnashai AS (2012) Probabilistic seismic performance assessment of code-compliant multi-story RC buildings. Eng Struct 34:527–537. https://doi.org/10.1016/j.engstruct.2011.10.019

Kassem MM, Mohamed Nazri F, Noroozinejad Farsangi E (2020) The seismic vulnerability assessment methodologies: a state-of-the-art review. Ain Shams Eng J 11:849–864. https://doi.org/10.1016/j.asej.2020.04.001

Kaya Y, Safak E (2019) Structural health monitoring: real-time data analysis and damage detection. Springer, pp 171–197

Kaya Y, Safak E (2015) Real-time analysis and interpretation of continuous data from structural health monitoring (SHM) systems. Bull Earthq Eng 13:917–934. https://doi.org/10.1007/s10518-014-9642-9
Kerschen G, Worden K, Vakakis AF, Golinval JC (2006) Past, present and future of nonlinear system identification in structural dynamics. Mech Syst Signal Process 20:505–592
Li Y, Song R, Van De Lindt JW (2014) Collapse fragility of steel structures subjected to earthquake mainshock-aftershock sequences. J Struct Eng 140:04014095. https://doi.org/10.1061/(ASCE)ST.1943-541X.0001019
Limongelli MP, Çelebi M (2019) Seismic structural health monitoring: from theory to successful applications. Springer, Cham
Luco N, Bazzurro P, Cornell AC (2004) Dynamic versus static computation of the residual capacity of a mainshock-damaged building to withstand an aftershock. In: 13th World conference on earthquake engineering
Omenzetter P, Limongelli MP, Yazgan U (2016) Quantifying the value of seismic structural health monitoring of buildings. In: 8th European workshop on structural health monitoring, EWSHM
Pozzi M, Der Kiureghian A (2011) Assessing the value of information for long-term structural health monitoring. In: Kundu T (ed) Health monitoring of structural and biological systems 2011. SPIE Press, San Diego, p 79842
Quqa S, Landi L, Diotallevi PP (2021) Seismic structural health monitoring using the modal assurance distribution. Earthq Eng Struct Dyn. https://doi.org/10.1002/eqe.3451
Raghunandan M, Liel AB, Luco N (2015) Aftershock collapse vulnerability assessment of reinforced concrete frame structures. Earthq Eng Struct Dyn 44:419–439. https://doi.org/10.1002/eqe.2478
Raghunandan M (2012) Influence of long duration ground shaking on collapse of reinforced concrete structures. University of Colorado
Raiffa H, Schlaifer R (1961) Applied statistical decision theory. Division of Research, Graduate School of Business Administration, Harvard University, Boston
Reasenberg PA, Jones LM (1989) Earthquake hazard after a mainshock in California. Science 243:1173–1176. https://doi.org/10.1126/science.243.4895.1173
Roohi M, Hernandez EM (2020) Performance-based post-earthquake decision making for instrumented buildings. J Civ Struct Health Monit 10:775–792. https://doi.org/10.1007/s13349-020-00416-1
Rossetto T, Elnashai A (2003) Derivation of vulnerability functions for European-type RC structures based on observational data. Eng Struct 25:1241–1263. https://doi.org/10.1016/S0141-0296(03)00060-9
Rupakhety R, Sigbjörnsson R (2009) Ground-motion prediction equations (GMPEs) for inelastic displacement and ductility demands of constant-strength SDOF systems. Bull Earthq Eng 7:661–679. https://doi.org/10.1007/s10518-009-9117-6
Ryu H, Luco N, Uma SR, Liel AB (2011) Developing fragilities for mainshock-damaged structures through incremental dynamic analysis. In: Proceedings of the ninth pacific conference on earthquake engineering, p 8
Shan J, Chen X, Yuan H, Shi W (2015) Interstory drift estimation of nonlinear structure using acceleration measurement with test validation. J Eng Mech 141:04015032. https://doi.org/10.1061/(ASCE)EM.1943-7889.0000950
Shiradhonkar SR, Shrikhande M (2011) Seismic damage detection in a building frame via finite element model updating. Comput Struct 89:2425–2438. https://doi.org/10.1016/j.compstruc.2011.06.006
Skolnik DA, Wallace JW (2010) Critical assessment of interstory drift measurements. J Struct Eng 136:1574–1584. https://doi.org/10.1061/(ASCE)ST.1943-541X.0000255
Straub D (2014) Value of information analysis with structural reliability methods. Struct Saf 49:75–85. https://doi.org/10.1016/j.strusafe.2013.08.006
Thöns S (2018) On the value of monitoring information for the structural integrity and risk management. Comput Aided Civ Infrastruct Eng 33:79–94. https://doi.org/10.1111/mice.12332
Thöns S, Stewart MG (2020) On the cost-efficiency, significance and effectiveness of terrorism risk reduction strategies for buildings. Struct Saf 85:101957. https://doi.org/10.1016/j.strusafe.2020.101957
Thöns S, Faber MH (2013) Assessing the value of structural health monitoring. In: Deodatis GG, Ellingwood BR, M.Frangopol D (eds) Safety, reliability, risk and life-cycle performance of structures and infrastructures—proceedings of the 11th international conference on structural safety and reliability ICOSSAR
Torfs T, Sterken T, Brebels S et al (2013) Low power wireless sensor network for building monitoring. IEEE Sens J 13:909–915. https://doi.org/10.1109/JSEN.2012.2218680
Tothong P, Luco N (2007) Probabilistic seismic demand analysis using advanced ground motion intensity measures. Earthq Eng Struct Dyn 36:1837–1860. https://doi.org/10.1002/eqe.696
Uma SR, Ryu H, Luco N, Liel AB, Raghunandan M (2011) Comparison of main-shock and aftershock fragility curves developed for New Zealand and US buildings. In: Proceedings of the ninth pacific conference on earthquake engineering: building an earthquake resilient society

UTSU T, (1970) Aftershocks and earthquake statistics(1): some parameters which characterize an aftershock sequence and their interrelations. J Fac Sci Hokkaido Univ 3:129–195

Verzobio A, Bolognani D, Quigley J, Zonta D (2021) Quantifying the benefit of structural health monitoring: can the value of information be negative? Struct Infrastruct Eng. https://doi.org/10.1080/15732479.2021.1890139

von Neumann J, Morgenstern O (1944) Theory of games and economic behaviour. Princeton University Press, Princeton

Wong SM, Onof CJ, Hobbs RE (2005) Models for evaluating the costs of bridge failure. Proc Instit Civ Eng Bridge Eng 158:117–128

Yeo GL (2005) Stochastic characterization and decision bases under time-dependent aftershock risk in performance-based earthquake engineering. Stanford University

Zhang W-H, Lu D-G, Qin J et al (2021) Value of information analysis in civil and infrastructure engineering: a review. J Infrastruct Preserv Resil 2:16. https://doi.org/10.1186/s43065-021-00027-0

Zonta D, Glisic B, Adriaenssens S (2014) Value of information: impact of monitoring on decision-making. Struct Control Health Monit 21:1043–1056. https://doi.org/10.1002/stc.1631